

Hybrid Antenna Array with the Bowtie Elements for Super-Resolution and 3D Scanning Radars

Somayeh Komeylian

Abstract—The antenna arrays for the entire 3D spherical coverage have been developed for their potential use in variety of applications such as radars and body-worn devices of the body area networks. In this study, we have rigorously revamped the hybrid antenna array using the optimum geometry of bowtie elements for achieving a significant improvement in the angular discrimination capability as well as in separating two adjacent targets. In this scenario, we have analogously investigated the effectiveness of increasing the virtual array length in fostering and enhancing the directivity and angular resolution in the 10 GHz frequency. The simulation results have extensively verified that the proposed antenna array represents a drastic enhancement in terms of size, directivity, side lobe level (SLL) and, especially resolution compared with the other available geometries. We have also verified that the maximum directivities of the proposed hybrid antenna array represent the robustness to the all θ variations, which is accompanied by the uniform 3D scanning characteristic.

Keywords—Bowtie antenna, hybrid antenna array, array signal processing, body area networks.

I. INTRODUCTION

THE main practical challenges of modern communication systems consist of the presence of obstacles of the long distance and interference signals of the traffic environments. An alternative way to overcome the aforementioned limitations involves steering the narrowest main radiation pattern in the direction of interest as well as directing nulls in the direction of not interest. In this scenario, the mainbeam characteristics and also the beam scanning capabilities of the antenna array are very much affected by the antenna array geometry. Among the various available 2D geometries of antenna arrays, the circular array establishes the superiority of providing continuous radiation pattern. Although the circular array does not have any edges or discontinuities, its performance still suffers from the high SLL and no nulls in the azimuthal plane. Concentric circular and concentric hexagonal arrays can significantly moderate the SLL; however they do not have any uniform directivity in the 3D space, [1]-[20]. In order to take full advantage of both cylindrical and concentric cylindrical arrays simultaneously, we have proposed a hybrid antenna array geometry in Fig. 1.

In practical scenario, especially in the traffic environments, high gain antenna systems are required to overcome higher propagation losses. However, a remarkable achievement to the accuracy and resolution in terms of both the range and the cross-angular direction limits the performance in a well-

Somayeh Komeylian is with the Ryerson University, Canada (e-mail: skomeylian1981@gmail.com).

designed radar system. Indeed, the range resolution, or the low value of ΔR in (1), refers to the capability of each radar system to discriminate between two or more targets in the same bearing, however in the different ranges.

$$\Delta R = \frac{c}{2B} \quad (1)$$

where c is the free-space velocity. B refers to the chirp bandwidth of the transmitted pulse.

An alternative way of fostering and enhancing the range accuracy and resolution consists of increasing the number of antenna elements. More antenna elements enable advanced signal processing techniques to represent the narrower mainbeam, and thereby to minimize clutters.

In this study, we have revamped the hybrid antenna array using the optimum geometry of the bowtie elements for achieving the high antenna gain and super-resolution. In addition, the radiation pattern of the bowtie antenna offers the high gain and directivity compared to its dipole counterpart.

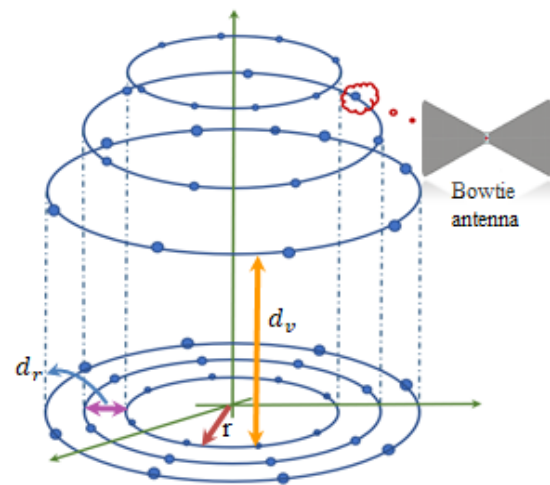


Fig. 1 The geometry of the hybrid antenna array comprises of cylindrical subarrays. Each cylindrical subarray is composed of two concentric circular subarrays positioned upon each other [2]. The implementation of the hybrid antenna array geometry will be fulfilled by the optimum bowtie array elements

II. DESIGN CONSIDERATION OF THE BOWTIE ANTENNA FOR THE HYBRID ANTENNA ARRAY

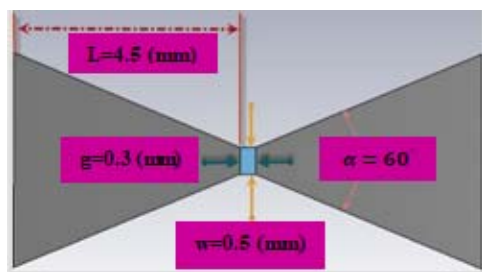
Each bowtie antenna is built of the two infinitesimal and conductive thin triangular segments, which are fed at the bow apex, Fig. 1. The potential use of the bowtie antenna in a variety of applications, [21]-[30], such as wireless

communications systems, radar systems, optical sensing, energy harvesting, and etc. is impelled by its unique features and advantages including near-field intensity enhancement, broad frequency bandwidth, and simple planar structure.

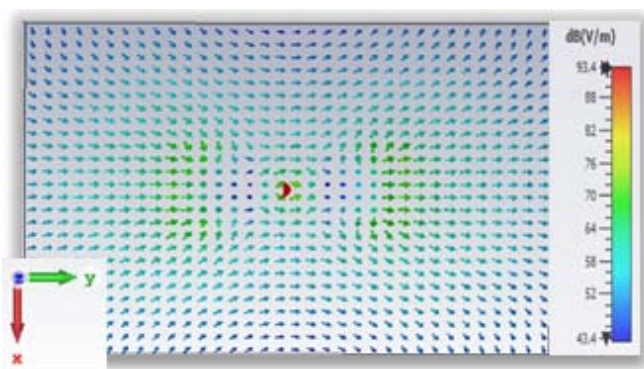
TABLE I

DESIGN PARAMETERS FOR THE PROPOSED HYBRID ANTENNA ARRAY

Parameters	Definition	Value
N	Number of elements of any circular loop	N = 20
Q	Number of elements of any cylinder	Q = 40
M	Total number of cylinders in the proposed array	M = 3
P	Number of circular loops in the cylinder	P = 2
d_v	Vertical spacing between two consecutive circular loops	$d_v = 0.5\lambda$
d_r	Horizontal spacing between two consecutive circular loops	$d_r = 0.5\lambda$
φ, θ	Maximum scanning angles	$\varphi = 0^\circ, \theta = 30^\circ$



(a)

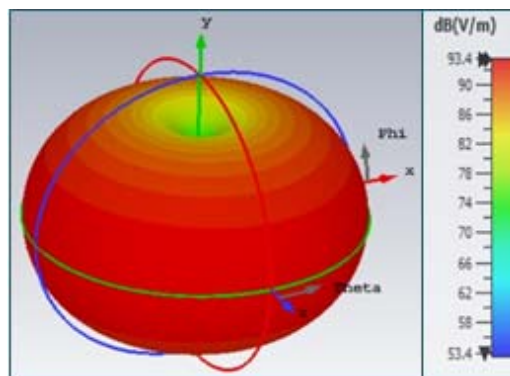


(b)

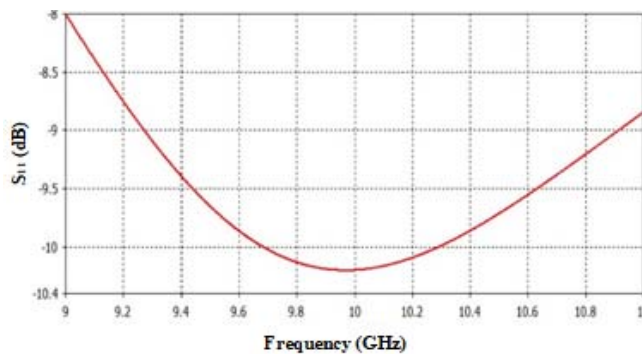
Fig. 2 The numerical results have been extensively fulfilled by the CST Studio simulation tool; (a) Top view of the optimum bowtie antenna with the thickness of 0.508 mm, (b) The electric field distribution on the surface of the optimum bowtie antenna at the 10 GHz frequency of the operation

Fig. 2 has reported that a high-intensity enhancement of the electric field is produced inside the feed gap of the bowtie antenna. The uniform broadband electric field has been significantly distributed over the entire bandgap. In other words, the bowtie antenna represents the maximum and uniform field distribution around its resonance frequency.

The 3D realized gain in Fig. 3 has demonstrated the low profile and directional ultra-wide band (UWB) radiation characteristics of the bowtie antenna, consistent with Fig. 2.



(a)



(b)

Fig. 3 (a) the radiation electric field of the optimum bowtie antenna, consistent with Fig. 2, fulfilled by CST Studio simulation tool at the frequency of operation of 10 GHz, (b) variation of S_{11} parameter versus frequency, which represents the frequency of operation of 10 GHz

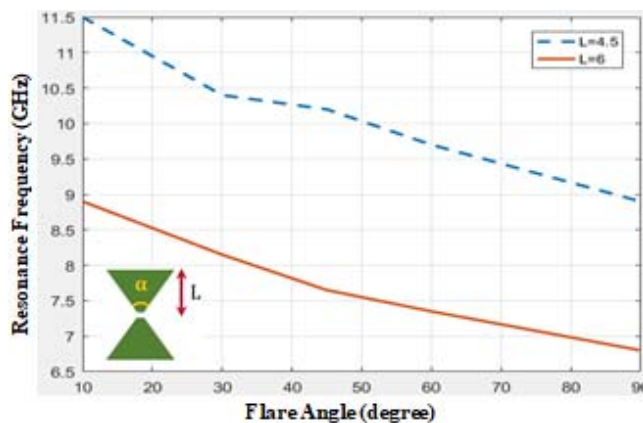


Fig. 4 Variation of resonance frequency of the bowtie element versus the flare angle for the two different arm lengths of $L = 4.5$ (mm) and $L = 6$ (mm). The other geometrical parameters of the bowtie element include the material type of Rogers RO4003C (lossy), $\epsilon_r = 3.38$, and $\mu_r = 1$. The substrate thickness is equal to 0.508 (mm)

It is worth mentioning that the resonance behavior of the bowtie antenna can be drastically adjusted by the geometrical parameters. In this scenario, the geometric shape of the bowtie antenna is indeed modified to enlarge by increasing its flare angle. The bowtie antenna with the longer arm length or the

higher flare angle allows flowing the current through the longer path to the gap and thereby the effective size of the antenna is increased. Any increase in the effective size of the antenna indeed is accompanied by the longer resonance wavelength and thereby the lower resonance frequency. Both Figs. 4 and 5 have analogously confirmed that the longer arm lengths or the greater flare angles are accompanied by the lower resonance frequencies.

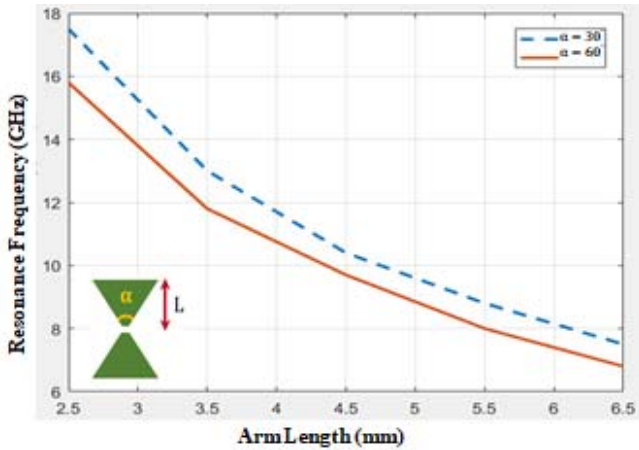


Fig. 5 Variation of resonance frequency of the bowtie element versus the arm lengths for the two different fixed flare angles of $\alpha = 30^\circ$ and $\alpha = 60^\circ$. The other geometrical parameters of the bowtie element are described in Fig. 4

III. ARRAY PATTERN SYNTHESIS OF THE HYBRID ANTENNA ARRAY

The discussion in the previous section focused on analyzing one array element of the bowtie antenna. In this section, we aim at implementing the proposed elements for the hybrid antenna array in Fig. 1.

Generally, the array pattern synthesis techniques are characterized by the two distinct scenarios; (1) the design of antenna array geometry for steering beampattern in an arbitrary direction in the space, (2) the implementation of beamforming techniques [1]-[13], for steering beampattern in the direction of interest in the space. In this section, the array signal processing technique has been focused on fostering and enhancing the performance of the hybrid antenna array using the bowtie antenna elements in response to increase necessity of the high resolution in the application of radars and wireless communications systems. The antenna array factor of the hybrid antenna array, consistent with Fig. 1, can be expanded by [2]:

$$AF = \sum_{n=1}^N I_n e^{jkr_0 \sin \theta \cos(\varphi - \varphi_n) + \alpha_n} + \sum_{m=1}^M \sum_{p=1}^2 \sum_{n=1}^N I_{mn} e^{j(p-1)(kd_m \cos \theta + \beta_m)} e^{jkr_m \sin \theta \cos(\varphi - \varphi_{mn})} \quad (2)$$

where the first term of AF refers to the array factor of the most outward circular ring located at the x-y plane. I_{mn} and I_n are magnitudes of excitations, which are supposed to be uniform.

φ_{mn} and β_m refer to the phase excitations.

In the scenario of deploying the hybrid antenna array with the bowtie elements, array parameters, including phase distribution, amplitude distribution, and spatial locations of array elements, are precisely simulated and assigned using the MATLAB simulation tool. Then, the text template of the array parameters is imported into the CST Studio simulation tool for analyzing the proposed geometry of the hybrid antenna array.

Fig. 6 represents the simulation results of implementing the bowtie antenna elements for the proposed geometry of the hybrid antenna array in Fig. 1 at the frequency of operation of 10 GHz. The realized gain in Fig. 6 has fully verified the superior performance of the hybrid antenna array in terms of steering and enhancing the mainbeam as well as fostering the resolution capability drastically. In other words, the innovation of implementing the hybrid antenna array using the bowtie elements provides the unique and exceptional characteristic of the high-directional realized gain of 56.3 dB compared with other available array geometries [1]-[18].

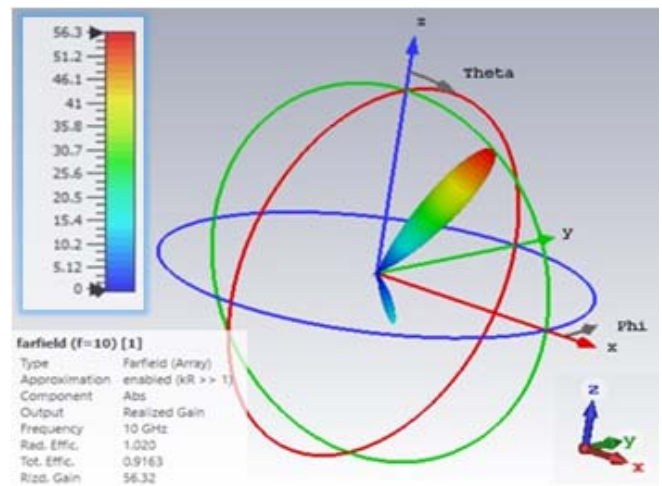


Fig. 6 Radiation electric field of deploying the hybrid antenna array using the optimum bowtie antenna elements at the frequency of operation of 10 GHz. The design parameters are represented in Figs. 2 and 3 and the number of the bowtie elements are supposed to be 14

IV. SUPER-RESOLUTION CAPABILITY OF THE HYBRID ANTENNA ARRAY

In the previous section, we have represented and evaluated the performance of the hybrid antenna array using the bowtie array elements in terms of directivity and resolution. In this section, we aim at investigating the effect of dense antenna array on steering mainlobe and thereby enhancing resolution. A densely spaced hybrid antenna array indeed allows achieving a significant increase in the virtual antenna array size and thereby a drastic improvement in the angular discrimination capability. In this scenario, the far field results have been obtained assuming the actual array length in the order of a few wavelengths or smaller. In this scenario, the densely spaced hybrid antenna array is employed to extrapolate the far field beyond the array extension for fostering and enhancing the angular resolution.

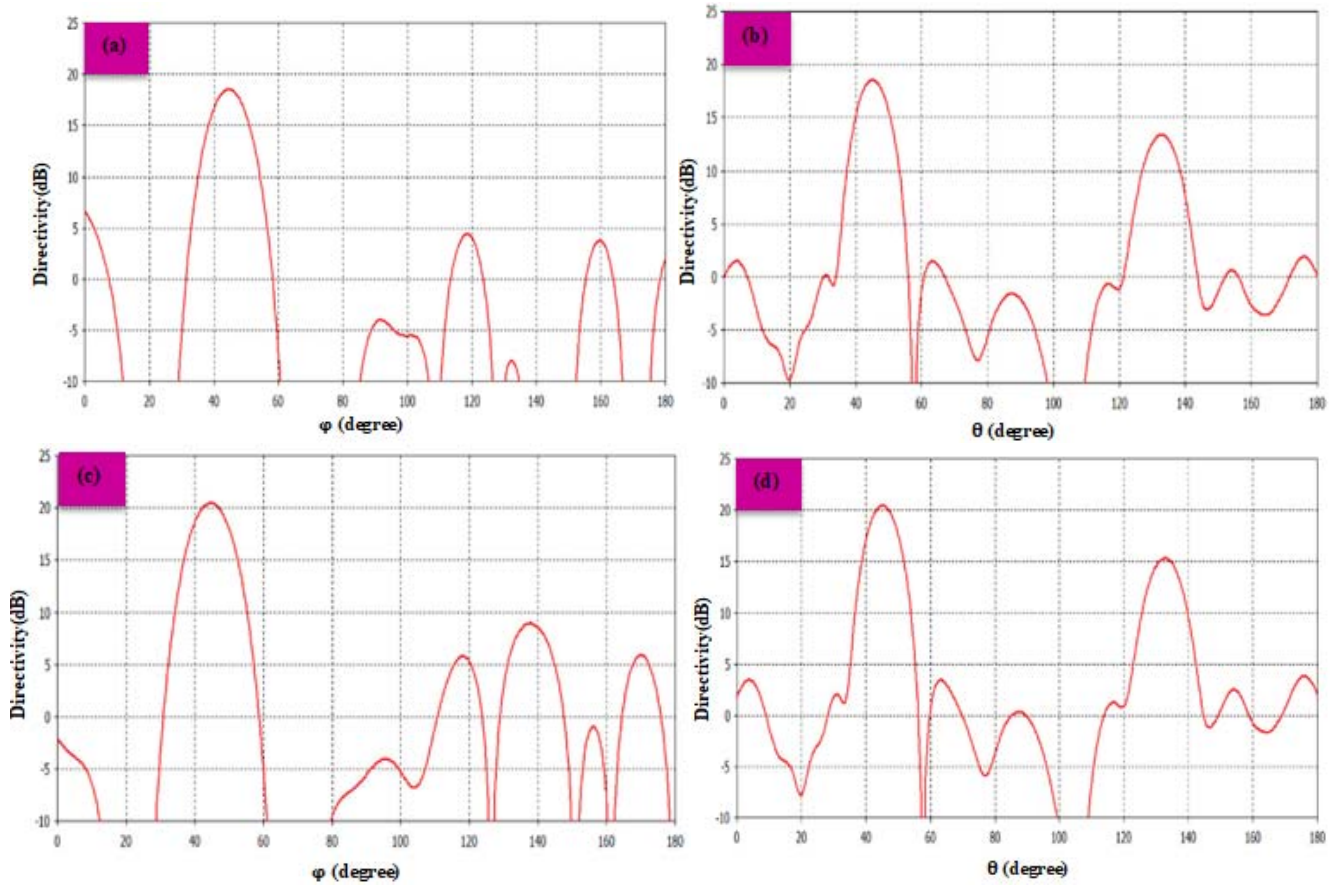


Fig. 7 Variation of directivity in the frequency of operation of 10 GHz for the proposed geometry of the hybrid antenna array in Fig. 1 and Table I, (a) $N = 10, M = 3, \theta = 45^\circ$, mainlobe magnitude = 18.5 dBi, 3 dB beamwidth = 11.7 deg., and SLL = -6.3 dB, (b) $N = 10, M = 3, \varphi = 45^\circ$, mainlobe magnitude = 18.5 dBi, 3 dB beamwidth = 9.9 deg., and SLL = -5.1 dB, (c) $N = 20, M = 3, \theta = 45^\circ$, mainlobe magnitude = 20.5 dBi, 3 dB beamwidth = 11.7 deg., and SLL = -11.5 dB, (d) $N = 20, M = 3, \varphi = 45^\circ$, mainlobe magnitude = 20.5 dBi, 3 dB beamwidth = 9.9 deg., and SLL = -5.1 dB

Analogously, Fig. 7 reported that the hybrid antenna array with the 140 bowtie elements has demonstrated better performance in terms of steering and enhancing the mainlobe in comparison with the hybrid antenna array with the 70 bowtie elements and with the same dimensions.

V.3D SCANNING CAPABILITY OF THE HYBRID ANTENNA ARRAY

The vital part of body-worn devices consists of employing an appropriate antenna [31], [32]. Since the antenna of each body-worn device should be located on the human body, the resonance frequency shifts and hence the antenna efficiency and gain drop. Consequently, the antenna radiation pattern will be distorted, especially in the presence of an undesired radiation towards the body.

The proposed hybrid antenna array of Fig. 1 can have a potential application for the body-worn devices and radars not only for its aforementioned advantages, in the previous sections, but also for its 3D scanning capability. In this section, we aim to validate and evaluate the 3D scanning characteristic of the proposed hybrid antenna array. The maximum directivities of the hybrid antenna array are

supposed to be equal for the whole variations of θ angles for the scenario of the uniform 3D scanning.

The maximum array factor can be obtained when the entire phase contribution to the array factor is identical to equal unity. Therefore, by satisfying the aforementioned condition in (2), the maximum array factor, in principle, is theoretically achieved when $d_v = 0.5\lambda$, $d_r = 0.5\lambda$, and $(\theta_0, \varphi_0) = (\approx 45^\circ, \approx 45^\circ)$. In this scenario, the maximum directivity in terms of the maximum array factor can be derived as follows,

$$D_0 = 4\pi \frac{|AF(\theta_0, \varphi_0)|^2}{\int_0^{2\pi} \int_0^\pi |AF(\theta, \varphi)|^2 \sin \theta d\theta d\varphi} \quad (3)$$

Simulation results of Fig. 8 have extensively verified that that the maximum directivity of the hybrid antenna array is fairly robust to changes and variations in different θ angles, which refers to its uniform 3D scanning capability.

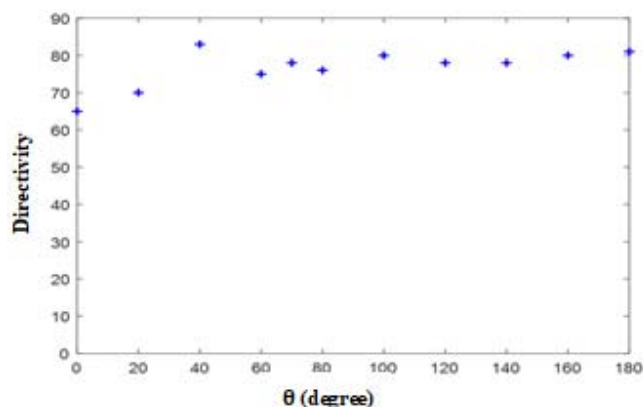


Fig. 8 The variation of maximum directivity versus θ angles at the same frequency of 10 GHz

VI. CONCLUSION

To conclude, in this study, we have rigorously implemented the hybrid antenna array using the bowtie elements for the radar applications. The proposed hybrid antenna array allows fostering and enhancing the directivity as well as reducing the spatial angle of the mainbeam, which are accompanied by improving the resolution capability of the radars significantly. In the following, we have represented that the spatial angle of the mainbeam and the antenna gain are very affected by the number of the array elements. In other words, any increase in the virtual length of the antenna array causes a significant enhancement in the hybrid antenna array performance in terms of its resolution capability. Furthermore, we have fully evaluated and validated the excellent 3D scanning performance of the proposed hybrid antenna array using MATLAB and CST Studio simulation tools.

This research has provided the reader a beneficial analysis to the hybrid antenna array and an insight into the future adaptive antenna arrays. Field programmable Gate Array (FPGA) hardware (HW) has been steadily increasing in the technical literature [33]-[37] for deploying the geometries of linear, circular, and cylindrical antenna arrays. The aforementioned technical literature [33]-[37] also ensures the possibilities for implementing the hybrid antenna array in realistic experimental setups, however, this work had a major contribution for synthesizing and analyzing radiation pattern.

REFERENCES

- [1] R. A. Sadeghzadeh, A. A. Lotfi Neyestanak, M. Naser-Moghadasi, and M. Ghiamy, "A Comparison of Various Hybrid Elliptical Antenna Arrays", *Iranian Journal of Electrical and Computer Engineering*, Vol. 7, No. 2, Summer-Fall 2008.
- [2] Mohammad Ghavami, "A Spatially Processed 3D Wideband Adaptive Conical Array System," 2017 IEEE 17th International Conference on Ubiquitous Wireless Broadband (ICUWB), 2017.
- [3] Najam-Us Saqib, Imdad Khan, "A Hybrid Antenna Array Design for 3-D Direction of Arrival Estimation," *PLoS ONE* 10(3): e0118914. doi:10.1371/journal. March 19, 2015.
- [4] Nasim Ebrahimi, Abbas Pirhadi, Majid Karimipour, "Optimum design of shaped beam cylindrical array antenna with electronically scan radiation pattern," *Advanced Computational Techniques in Electromagnetics* 2013 (2013) 1-11, 2013.
- [5] Elias Yaacoub, Mohammed Al-Husseini, Ali Chehab, Karim Y. Kabalan, Ali El-Hajj "Pattern Synthesis with Cylindrical Arrays,"

- ResearchGate, 2006.
- [6] Bindong Gao, Fangzheng Zhang, Ermao Zhao, Daocheng Zhang, And Shilong Pan, "High-Resolution Phased Array Radar Imaging by Photonics-Based Broadband Digital Beamforming," 27, No. 9 | 29 Apr 2019 | *Optics Express* 13194.
- [7] Sangwook Kim, Swathi Kavuri, and Minho Lee, "Deep Network with Support Vector Machines," M. Lee et al. (Eds.): *ICONIP 2013, Part I*, LNCS 8226, pp. 458–465, Springer-Verlag Berlin Heidelberg, 2013.
- [8] Gonzalo Acuña and Millaray Curilem, "Comparison of Neural Networks and Support Vector Machine Dynamic Models for State Estimation in Semiautogenous Mills," A. Hernández Aguirre et al. (Eds.): *MICAI 2009, LNAI 5845*, pp. 478–487, Springer-Verlag Berlin Heidelberg 2009.
- [9] Yue Wu, Hui Wang, Biaobiao Zhang, and K.-L. Du, "Using Radial Basis Function Networks for Function Approximation and Classification," *International Scholarly Research Network, ISRN Applied Mathematics*, Volume 2012, Article ID 324194, 34 pages, doi:10.5402/2012/324194.
- [10] JAK Suykens, J De Brabanter, L Lukas, J Vandewalle, "Neurocomputing, Weighted least squares support vector machines: robustness and sparse approximation," Elsevier, 2002.
- [11] A. W. Jayawardena, D. A. K. Fernando & M. C. Zhou, "Comparison of Multilayer Perceptron and Radial Basis Function networks as tools for flood forecasting," *Destructive Water: Water-Caused Natural Disasters, their Abatement and Control (Proceedings of the Conference held at Anaheim, California, June 1996)*. IAHS Publ. no. 239, 1997.
- [12] Judd A. Rohwer and Chaouki T. Abdallah, "One-vs-One Multiclass Least Squares Support Vector Machines for Direction of Arrival Estimation", *Aces Journal*, Vol. 18, No. 2, July 2003.
- [13] Marija Agatonović, Zoran Stanković, Bratislav Milovanović, and Nebojša Dončov, "DOA Estimation using Radial Basis Function Neural Networks as Uniform Circular Antenna Array Signal Processor," *International Conference on Telecommunications in Modern Satellite, Cable and Broadcasting Service (TELSIKS)*, 2011.
- [14] Yu.B. Nechaev, I.W. Peshkov, N.A. Fortunova, "Cylindrical antenna array development and measurements for DOA-estimation applications," 2017 XI International Conference on Antenna Theory and Techniques (ICATT), 2017.
- [15] Monther Abusultan, Sam Harkness, Brock J. LaMeres, and Yikun Huang, "FPGA implementation of a Bartlett direction of arrival algorithm for a 5.8ghz circular antenna array," 2010 IEEE Aerospace Conference.
- [16] Abdallah, Chaouki T., Judd A. Rohwer, and Christos G. Christodoulou., "Least squares support vector machines for direction of arrival estimation with error control and validation," *IEEE Global Telecommunications Conference (2003)*: 2172-2176. doi:10.1109/GLOCOM.2003.
- [17] Yugo M. KUNO, Bruno MASIERO, and Nilesh MADHU, "A neural network approach to broadband beamforming," *ICA2019, the 23rd International Congress and Acoustics*, 2019.
- [18] Lei Wang, "Array Signal Processing Algorithms for Beamforming and Direction Finding," Ph.D. thesis of University of York, 2009.
- [19] Zhang-Meng Liu, Chenwei Zhang and Philip S. Yu, "Direction-of-Arrival Estimation based on Deep Neural Networks with Robustness to Array Imperfections," *IEEE Transactions on Antennas and Propagation*, 2018.
- [20] Somayeh Komeyliyan, "Implementation and Evaluation of LS-SVM Optimization Methods for Estimating DoAs," *IEEE CCECE* 2020.
- [21] Xingyu Zhang, Chi-Jui Chung, Shiyi Wang, Harish Subbaraman, Zeyu Pan, Qiwen Zhan, and Ray T. Chen, "Integrated Broadband Bowtie Antenna on Transparent Silica Substrate," *IEEE Antennas and Wireless Propagation Letters*, Vol. 15, 2016.
- [22] R. C. Compton et al., "Bow-tie antennas on a dielectric half-space: Theory and experiment," *IEEE Trans. Antennas Propag.*, vol. AP-35, no. 6, pp. 622–631, Jun. 1987.
- [23] S. Kim et al., "High-harmonic generation by resonant plasmon field enhancement," *Nature*, Vol. 453, pp. 757–760, 2008.
- [24] K. D. Ko et al., "Nonlinear optical response from arrays of Au bowtie nanoantennas," *Nano Lett.*, vol. 11, pp. 61–65, 2010.
- [25] B. Madhav et al., "Liquid crystal bow-tie microstrip antenna for wireless communication applications," *J. Eng. Sci. Technol. Rev.*, vol.4, pp.131–134, 2011.
- [26] Z. Pan and J. Guo, "Enhanced optical absorption and electric field resonance in diabolical metal bar optical antennas," *Opt. Exp.*, vol.21, pp.32491–32500, 2013.

- [27] M. Rahim, M. Abdul Aziz, and C. Goh, "Bow-tie microstrip antenna design," in Proc. 13th IEEE Int. Conf. Netw., 2005.
- [28] M. Roslee, K. S. Subari, and I. S. Shahdan, "Design of bow tie antenna in CST studio suite below 2 GHz for ground penetrating radar applications," Proc. IEEE RFM, pp. 430–433, 2011.
- [29] S. Sederberg and A. Elezzabi, "Nanoscale plasmonic contour bowtie antenna operating in the mid-infrared," Opt. Exp., vol. 19, pp. 15532–15537, 2011.
- [30] C. A. Balanis, Antenna theory: Analysis and design. Hoboken, NJ, USA: Wiley, 2012.
- [31] F. I. Rial, H. Lorenzo, M. Pereira, and J. Armesto, "Analysis of the emitted wavelet of high-resolution bowtie GPR Antennas," Sensors, vol. 9, pp. 4230–4246, 2009.
- [32] Adedayo Omisakin, "Metamaterial AMC backed Antenna for Body-worn Application at 2.4GHz," Thesis for the Master of Science in Eindhoven University of Technology, 2017.
- [33] G. Naldi, M. Bartolini, A. Mattana, G. Pupillo, J. Hickish, G. Foster, G. Bianchi, A. Lingua, J. Monari, S. Montebugnoli, F. Perini, S. Rusticelli, M. Schiaffino, G. Virone, and K. Zarb Adami, "Developments of FPGA-based digital back-ends for low frequency antenna arrays at Medicina radio telescopes," Mem. S.A. It. Vol.88, 206 SA It, 2017.
- [34] Vinayak Nagpal, "An FPGA Based Phased Array Processor for the Sub-Millimeter Array," Chalmers University of Technology, Gothenburg, Sweden Harvard Smithsonian Center for Astrophysics, Cambridge, MA, September 2005.
- [35] Miroslav Joler, "How FPGAs Can Help Create Self-Recoverable Antenna Arrays," International Journal of Antennas and Propagation, 2012.
- [36] Ahmed A. Hussain, Nizar Tayem, Saleh A. Alshebeili, "FPGA Hardware Implementation of DOA Estimation Algorithm Employing LU Decomposition," Published in IEEE Access 2018.
- [37] Monther Abusultan, Sam Harkness, Brock J. La Meres, and Yikun Huang, "FPGA implementation of a Bartlett direction of arrival algorithm for a 5.8GHz circular antenna array," IEEE Aerospace Conference Proceedings, April 2010.